Solitary-pulse stabilization and shortening in actively mode-locked lasers

F. X. Kärtner, D. Kopf, and U. Keller

Institute of Quantum Electronics, Swiss Federal Institute of Technology, Ultrafast Laser Physics Laboratory, ETH Hönggerberg HPT, CH-8093 Zürich, Switzerland

Received April 15, 1994; revised manuscript received September 27, 1994

We present a theory and experiments on active mode locking in the presence of negative group-velocity dispersion (GVD) and self-phase modulation (SPM). It is shown that beyond a critical value of GVD a solitonlike pulse can be stabilized by the mode locker. The width of the soliton can be shorter than the width of the Gaussian pulse produced by the mode locker in the absence of soliton shaping. We establish analytically that the pulse shortening possible by addition of SPM and GVD is limited only by the requirement that the phase shift of the soliton per round trip be limited. Parameter ranges allowing for stable solitary-pulse formation and shortening are derived and discussed for different gain media and compared with numerical simulations and experimental results.

1. INTRODUCTION

It has been well known for quite some time that the addition of a nonlinear index medium to a passively or actively mode-locked laser system may lead to shorter pulses.[1] The bandwidth limitation that results from gain dispersion can be partially overcome by the spectral broadening caused by the nonlinearity. However, as has been shown by the numerical simulations of Haus and Silberberg,[1] pulse shortening in an actively mode-locked system is limited by roughly a factor of 2 in the case of self-phase modulation (SPM) only. They also showed that the addition of negative group-velocity dispersion (GVD) can undo the chirp introduced by SPM, and therefore both effects together may lead to stable pulse shortening by a factor of 2.5.

Experimental results with fiber lasers[2–4] and solid-state lasers[5,6] indicate that soliton shaping in the negative GVD regime may lead to pulse stabilization and considerable pulse shorting. In this paper we extend the analysis of Haus and Silberberg by investigating the possible reduction in pulse width of an actively mode-locked laser as a result of solitonlike pulse formation, i.e., the presence of SPM and an excessive amount of negative GVD. We show by means of soliton perturbation theory that beyond a critical amount of negative GVD a solitonlike pulse is formed and kept stable by an active mode locker.

If the bandwidth of the gain is large enough, the width of this solitary pulse can be much less than the width of a Gaussian pulse generated by the active mode locker and gain dispersion alone. We establish analytically that the pulse shortening possible by addition of SPM and GVD does not have a firm limit of 2.5. These analytical results are confirmed by numerical simulations and experiments with a regeneratively actively mode-locked Nd:glass laser.

The pulse-width reduction achievable depends on the amount of negative GVD available. For an actively mode-locked Nd:glass laser a pulse shortening up to a factor of 6 may result, until instabilities arise. Indeed, if additional intracavity filtering is properly applied, femtosecond pulses can be achieved with an actively mode-locked Nd:glass laser, as was observed recently[6] and is now explained theoretically. The Nd:glass laser was one of the first solid-state lasers used for ultrashort-pulse generation[7] and is still interesting because it can be diode pumped.[8,9] The technique established in this paper may allow for efficient diode-pumped actively mode-locked Nd:glass lasers producing 1.5-ps or even femtosecond pulses, which can be used efficiently to pump optical parametric oscillators or seed amplifiers. This theory is also applicable to actively mode-locked fiber lasers in the negative-dispersion regime, where soliton formation plays a dominant role.[2–4]

2. ACTIVE MODE LOCKING AND SOLITON PERTURBATION THEORY

Pulse evolution in an actively mode-locked laser system with SPM and GVD is described by the master equation of mode locking of Haus and co-workers[1,10,11]:

$$T_R \frac{\partial A(T,t)}{\partial T} = -iD \frac{\partial^2 A}{\partial t^2} + i\delta |A|^2 A + \left\{ g\left(1 + \frac{1}{\Omega_g{}^2} \frac{\partial^2}{\partial t^2}\right) - l - M[1 - \cos(\omega_M t)] \right\} A \quad (2.1)$$

if the change in the pulse per round trip is small. We have assumed that the modulator is always perfectly matched to the round-trip frequency of the pulse in the cavity, a condition achievable by regenerative mode locking. We denote by $A(T, t)$ the slowly varying envelope of the pulse; T is a coarse-grained time that develops on a time scale of the order of the round-trip time T_R in the cavity, t denotes the fast time scale of the order of the pulse width, D is the intracavity dispersion per round trip, l is the loss per round trip, M is the modulation depth, and ω_M is the modulation frequency. g is the saturated gain of the laser medium, which is given by

0740-3224/95/030486-11$06.00

$$g = \frac{g_0}{1 + (W/E_L)}, \tag{2.2}$$

with the pulse energy

$$W = \int_{-T_R/2}^{T_R/2} |A(T, t)|^2 \mathrm{d}t, \tag{2.3}$$

and where g_0 denotes the unsaturated gain and E_L the saturation energy of the laser medium. As is evident from the formulation we assume a gain medium with a long relaxation time and a large saturation energy, so that the gain is appreciably saturated only by a series of successive pulses traveling through the gain medium; i.e., we can neglect dynamic gain saturation. This is usually the case in most solid-state lasers. There are no analytic solutions to the full master equation (2.1). However, without the dissipative effects, i.e., gain, loss, and modulation, the resulting equation is the nonlinear Schrödinger equation (NSE) exhibiting soliton solutions.[12]

A. Soliton of the NSE

In case of negative GVD, the NSE possesses soliton solutions. The general fundamental soliton solution is given by

$$A_s(T, t) = A_0 \operatorname{sech}(x)\exp(i\theta), \tag{2.4}$$

with

$$x = (1/\tau)(t - 2|D|p_0 T - t_0) \tag{2.5}$$

and the nonlinear phase shift

$$\theta = p_0(t - t_0) + |D|\left(\frac{1}{\tau^2} - {p_0}^2\right)T + \theta_0, \tag{2.6}$$

where we have introduced the initial frequency offset p_0 from the assumed carrier frequency, initial time t_0, and phase θ_0. The balance between GVD and SPM is achieved when the chirp introduced by the nonlinear phase shift is compensated for by GVD, which leads to

$$\Phi_0 = \tfrac{1}{2}\,\delta {A_0}^2 = \frac{|D|}{\tau^2}, \tag{2.7}$$

where Φ_0 denotes the phase shift of the soliton per round trip through the cavity. The energy contained in the soliton is given by

$$W = \int_{-\infty}^{\infty} |A_s(T, t)|^2 \mathrm{d}t = 2{A_0}^2\tau. \tag{2.8}$$

B. Active Mode Locking without GVD and SPM

Active mode locking without GVD and SPM has been studied analytically by Kuizenga and Siegman[13] with the circulating Gaussian pulse analysis and by Haus[10] in the framework of the master equation (2.1). The results of Ref. 10 are crucial for understanding of the following analysis and are therefore briefly summarized.

In the absence of GVD and SPM the mode-locking process is described by

$$T_R \frac{\partial A}{\partial T} = \left\{ g\left(1 + \frac{1}{{\Omega_g}^2}\frac{\partial^2}{\partial t^2}\right) - l - M[1 - \cos(\omega_M t)]\right\} A. \tag{2.9}$$

Assuming a certain pulse energy W and thus a fixed saturated gain, Eq. (2.9) is a linear partial differential equation that can be solved by separation of variables. Furthermore, the pulses that we expect to result will have a width much shorter than the round-trip time in the cavity and will be placed in time at the position where the modulator introduces the least loss. Thus we can approximate the cosine by a parabola and obtain the eigensolutions

$$A_n(T, t) = A_n(t)\exp(\lambda_n T/T_R), \tag{2.10}$$

$$A_n(t) = [W_n/(2^n\sqrt{\pi}\, n!\, \tau_a)]^{1/2} \times H_n(t/\tau_a)\exp\left(-\frac{t^2}{2{\tau_a}^2}\right), \tag{2.11}$$

where τ_a is the pulse width of the Gaussian, given by

$$\tau_a = \sqrt[4]{D_g/M_s}, \tag{2.12}$$

and D_g denotes the gain dispersion and M_s the modulator strength:

$$D_g = \frac{g}{{\Omega_g}^2}, \tag{2.13}$$

$$M_s = \frac{M{\omega_M}^2}{2}. \tag{2.14}$$

The round-trip gain of the eigenmode considered is given by its eigenvalue (or in general by the real part of the eigenvalue), which is given by

$$\lambda_n = g_n - l - 2M_s{\tau_a}^2(n + \tfrac{1}{2}), \tag{2.15}$$

where

$$g_n = \frac{1}{1 + (W_n/E_L)}. \tag{2.16}$$

From Eq. (2.15) we see that for a given pulse energy the mode with $n = 0$, which we call the ground mode, has the largest eigenvalue. Consequently the ground mode experiences the highest gain per round trip, because it has the narrowest spectrum compared with all the other modes and represents at the same time the shortest pulse in comparison with the other modes. Thus, starting with an arbitrary pulse shape, the ground mode will see the highest gain per round trip and saturates the gain to a value so that $\lambda_0 = 0$ in steady state and therefore suppresses all other modes $\lambda_n < 0$ for $n \geq 1$. This proves the stability of the ground mode.[10] Thus active mode locking produces Gaussian pulses with a FWHM given by

$$\tau_{a,\mathrm{FWHM}} = 1.66\tau_a. \tag{2.17}$$

In Subsection 2.C we use soliton perturbation theory to derive the requirements on the strength of SPM and GVD to transform the Gaussian pulse from the active mode locker into a stable soliton.

C. Soliton Perturbation Theory

In the presence of negative GVD and SPM the interplay between GVD and SPM will tend to form a sech-shaped pulse with a constant phase over the pulse, similar to the fundamental soliton of NSE (2.4). Therefore we will call this pulse a soliton despite the fact that, in the strict sense of definition, it is only a solitary wave.

In what follows, we derive the requirements for the strength of SPM and GVD such that the Gaussian pulse formed by the mode locker is transformed into a stable soliton by means of soliton perturbation theory. Soliton perturbation theory has been successfully used to study the influence of loss, filtering, the action of an active mode locker, periodic perturbations, and noise on a soliton.[11,14–18] In contrast, here we derive a self-consistent equation for the soliton and the continuum contribution that form the new solitary pulse. This is an approximate solution of Eq. (2.1), which assumes a small contribution from the continuum. It allows us to determine the parameter ranges of stable soliton generation.

Starting from the fundamental soliton solution [Eq. (2.4)], we assume that the solution of the full master equation (2.1) can be solved by the ansatz

$$A(T, t) = [a(x) + a_c(T, t)]\exp(i\theta + \Delta p t), \tag{2.18}$$

with

$$a(x) = A\ \mathrm{sech}(x), \qquad x = (1/\tau)[t - \Delta t(T)], \tag{2.19}$$

where a_c is the continuum that we will characterize below in more detail.[17] We also allow for a continuous change in the soliton amplitude A or energy $W = 2A^2\tau$ and small corrections of the soliton parameters phase $\Delta\theta$, carrier frequency Δp, and timing Δt; that is,

$$\theta = \frac{1}{T_R}\int_0^T \Phi(T')\mathrm{d}T' + \Delta\theta(T), \tag{2.20}$$

with

$$\Phi = |D|/\tau^2 = \delta A^2/2. \tag{2.21}$$

However, we assume changes in carrier frequency and timing. Introducing Eq. (2.18) into Eq. (2.1) and keeping terms in first order, we obtain for the perturbations the equation

$$\begin{aligned} T_R\left[\frac{\partial \mathbf{a}_c}{\partial T} + \frac{\partial W}{\partial T}\mathbf{f}_w + \frac{\partial \Delta\theta}{\partial T}\mathbf{f}_\theta + \frac{\partial \Delta p}{\partial T}\mathbf{f}_p + \frac{\partial \Delta t}{\partial T}\mathbf{f}_t\right] \\ = \Phi\mathbf{L}(\mathbf{a}_c + \Delta p\mathbf{f}_p) + \mathbf{R}(\mathbf{a} + \Delta p\mathbf{f}_p + \mathbf{a}_c) \\ - M\omega_M\ \sin(\omega_M\tau x)\Delta t\mathbf{a}(x). \end{aligned} \tag{2.22}$$

Note that the NSE couples the complex amplitude to its complex conjugate, which necessitates the introduction of the vector notation. The last term arises because the active mode locker breaks the time invariance of the system and leads to a restoring force pushing the soliton back to its equilibrium position.[14] The vector $\mathbf{a}_c$ is determined by (a_c, a_c^*) and $\mathbf{a}$ analogously. $\mathbf{L}$ and $\mathbf{R}$ are the operators of the linearized NSE and the active mode-locking equation, respectively:

$$\mathbf{L} = i\boldsymbol{\sigma}_3\left[\left(\frac{\partial^2}{\partial x^2} - 1\right) + 2\ \mathrm{sech}^2(x)(2 + \boldsymbol{\sigma}_1)\right], \tag{2.23}$$

$$\mathbf{R} = g\left(1 + \frac{1}{\Omega_g{}^2\tau^2}\frac{\partial^2}{\partial x^2}\right) - l - M[1 - \cos(\omega_M\tau x)], \tag{2.24}$$

$\boldsymbol{\sigma}_i$, $i = 1, 2, 3$ are the Pauli matrices, and the vectors $\mathbf{f}_w$, $\mathbf{f}_\theta$, $\mathbf{f}_p$, and $\mathbf{f}_t$ describe the change in the soliton when the soliton energy, phase, carrier frequency, and timing vary:

$$\mathbf{f}_w(x) = \frac{1}{W}[1 - x\ \tanh(x)]a(x)\begin{pmatrix}1\\1\end{pmatrix}, \tag{2.25}$$

$$\mathbf{f}_\theta(x) = ia(x)\begin{pmatrix}1\\-1\end{pmatrix}, \tag{2.26}$$

$$\mathbf{f}_p(x) = ix\tau a(x)\begin{pmatrix}1\\-1\end{pmatrix}, \tag{2.27}$$

$$\mathbf{f}_t(x) = \frac{1}{\tau}\tanh(x)a(x)\begin{pmatrix}1\\1\end{pmatrix}. \tag{2.28}$$

The action of the evolution operator of the linearized NSE on the soliton perturbations is

$$\mathbf{L}\mathbf{f}_w = \frac{1}{W}\mathbf{f}_\theta, \tag{2.29}$$

$$\mathbf{L}\mathbf{f}_\theta = 0, \tag{2.30}$$

$$\mathbf{L}\mathbf{f}_p = -2\tau^2\mathbf{f}_t, \tag{2.31}$$

$$\mathbf{L}\mathbf{f}_t = 0. \tag{2.32}$$

Equations (2.29) and (2.31) denote that perturbations in energy and carrier frequency are converted into additional phase and timing fluctuations of the pulse as a result of SPM and GVD. The full continuous spectrum of the linearized NSE has been studied by Kaup[17] and is given by

$$\mathbf{L}\mathbf{f}_k = \lambda_k\mathbf{f}_k, \tag{2.33}$$

$$\lambda_k = -i(k^2 + 1), \tag{2.34}$$

$$\mathbf{f}_k(x) = \exp(ikx)\begin{pmatrix}(k + i\ \tanh\ x)^2\\ \mathrm{sech}^2\ x\end{pmatrix}, \tag{2.35}$$

$$\mathbf{L}\bar{\mathbf{f}}_k = \bar{\lambda}_k\bar{\mathbf{f}}_k, \tag{2.36}$$

$$\bar{\lambda}_k = +i(k^2 + 1), \tag{2.37}$$

$$\bar{\mathbf{f}}_k = \boldsymbol{\sigma}_1\mathbf{f}_k. \tag{2.38}$$

Our definition of the eigenfunctions is slightly different from that of Kaup for reasons that will become obvious below. In contrast to Kaup,[17] we define the inner product in the complex space as

$$\langle\mathbf{u}\,|\,\mathbf{v}\rangle = \frac{1}{2}\int_{-\infty}^{+\infty}\mathbf{u}^+(x)\mathbf{v}(x)\mathrm{d}x. \tag{2.39}$$

With this definition, the inner product of a vector with itself in the subspace where the second component is the

complex conjugate of the first component is the energy of the signal, a physical quantity.

With respect to this inner product, $i\mathbf{L}$ is not self-adjoint, because the linearized system does not conserve energy as a result of the parametric pumping by the soliton. However, from Eqs. (2.23) and (2.39) we can easily see that the adjoint operator is now given by

$$\mathbf{L}^{+} = -\boldsymbol{\sigma}_3 \mathbf{L} \sigma_3 , \tag{2.40}$$

and therefore we get

$$\mathbf{L}^{+}\mathbf{f}_k^{(+)} = \lambda_k^{(+)}\mathbf{f}_k^{(+)}, \tag{2.41}$$

$$\lambda_k^{(+)} = -i(k^2 + 1), \tag{2.42}$$

$$\mathbf{f}_k^{(+)} = \frac{1}{\pi(k^2+1)^2}\,\boldsymbol{\sigma}_3 \bar{\mathbf{f}}_k ; \tag{2.43}$$

$$\mathbf{L}^{+}\bar{\mathbf{f}}_k^{(+)} = \bar{\lambda}_k^{(+)}\bar{\mathbf{f}}_k^{(+)}, \tag{2.44}$$

$$\bar{\lambda}_k^{(+)} = i(k^2 + 1), \tag{2.45}$$

$$\bar{\mathbf{f}}_k^{(+)} = -\frac{1}{\pi(k^2+1)^2}\,\boldsymbol{\sigma}_3 \mathbf{f}_k . \tag{2.46}$$

The eigenfunctions to $\mathbf{L}$ and its adjoint are mutually orthogonal:

$$\langle \mathbf{f}_k^{(+)} | \mathbf{f}_{k'} \rangle = \delta(k - k'), \qquad \langle \bar{\mathbf{f}}_k^{(+)} | \bar{\mathbf{f}}_{k'} \rangle = \delta(k - k'),$$
$$\langle \bar{\mathbf{f}}_k^{(+)} | \mathbf{f}_{k'} \rangle = \langle \mathbf{f}_k^{(+)} | \bar{\mathbf{f}}_{k'} \rangle = 0 .$$

We make this system, which describes the continuum excitations, complete by also taking into account the perturbations of the four degrees of freedom of the soliton, Eqs. (2.25)–(2.28):

$$\mathbf{f}_w^{(+)}(x) = -i2\tau\boldsymbol{\sigma}_3\mathbf{f}_\theta(x) = 2\tau a(x)\begin{pmatrix} 1 \\ 1 \end{pmatrix}, \tag{2.47}$$

$$\mathbf{f}_\theta^{(+)}(x) = 2i\tau\boldsymbol{\sigma}_3\mathbf{f}_w(x) = \frac{2i\tau}{W}[1 - x\tanh(x)]a(x)\begin{pmatrix} 1 \\ -1 \end{pmatrix}, \tag{2.48}$$

$$\mathbf{f}_p^{(+)}(x) = \frac{2i\tau}{W}\,\boldsymbol{\sigma}_3\mathbf{f}_t(x) = \frac{2i}{W}\tanh(x)a(x)\begin{pmatrix} 1 \\ -1 \end{pmatrix}, \tag{2.49}$$

$$\mathbf{f}_t^{(+)}(x) = \frac{-2i\tau}{W}\,\boldsymbol{\sigma}_3\mathbf{f}_p(x) = \frac{2\tau^2}{W}\,xa(x)\begin{pmatrix} 1 \\ 1 \end{pmatrix}. \tag{2.50}$$

Then the unity can be decomposed into two projections, one onto the continuum and one onto the perturbation of the soliton[17]:

$$\delta(x - x') = \int_{-\infty}^{\infty} \mathrm{d}k[|\mathbf{f}_k\rangle\langle\mathbf{f}_k^{(+)}| + |\bar{\mathbf{f}}_k\rangle\langle\bar{\mathbf{f}}_k^{(+)}|] + |\mathbf{f}_w\rangle\langle\mathbf{f}_w^{(+)}| + |\mathbf{f}_\theta\rangle\langle\mathbf{f}_\theta^{(+)}| + |\mathbf{f}_p\rangle\langle\mathbf{f}_p^{(+)}| + |\mathbf{f}_t\rangle\langle\mathbf{f}_t^{(+)}| . \tag{2.51}$$

From Eqs. (2.18) and (2.51) we can see that a_c is the continuum that then can be decomposed as

$$\mathbf{a}_c = \int_{-\infty}^{\infty} \mathrm{d}k[\, g(k)|\mathbf{f}_k\rangle + \bar{g}(k)|\bar{\mathbf{f}}_k\rangle] . \tag{2.52}$$

Note that the continuum $\mathbf{a}_c$ has to lie in the subspace defined by

$$\boldsymbol{\sigma}_1\mathbf{a}_c = \mathbf{a}_c^{*} , \tag{2.53}$$

and therefore the spectra of the continuum $g(k)$ and $\bar{g}(k)$ have to be related by

$$\bar{g}(k) = g(-k)^{*} . \tag{2.54}$$

Then we can directly compute the continuum from its spectrum, using Eqs. (2.35), (2.52), and (2.53):

$$a_c = -\frac{\partial^2 G(x)}{\partial x^2} + 2\tanh(x)\frac{\partial G(x)}{\partial x} - \tanh^2(x)G(x) + G^{*}(x)\mathrm{sech}^2(x) , \tag{2.55}$$

where $G(x)$ is up to the phase factor $\exp(i\theta)$ Gordon's associated function,[15] which is the inverse Fourier transform of the spectrum:

$$G(x) = \int_{-\infty}^{\infty} g(k)\exp(ikx)\mathrm{d}k . \tag{2.56}$$

3. SOLITON STABILIZATION BY ACTIVE MODE LOCKING

In this section we prove that a stable soliton can exist in the presence of the mode locker and of gain dispersion if the ratio between the negative GVD and the gain dispersion is sufficient. From Eq. (2.22) we obtain the equations of motion for the soliton parameters and the continuum by projecting out with the corresponding adjoint functions. Specifically, for the soliton energy we get

$$T_R\,\frac{\partial W}{\partial T} = 2\left(g - l - \frac{g}{3\Omega_g{}^2\tau^2} - \frac{\pi^2}{24}M\omega_M{}^2\tau^2\right)W + \langle \mathbf{f}_w^{(+)} | \mathbf{R}\mathbf{a}_c \rangle . \tag{3.1}$$

We see that gain saturation does not lead to a coupling between the soliton and the continuum to first order in the perturbation. Because the soliton and the continuum are orthogonal to each other in the sense of Eq. (2.39), to first order the total field energy is contained in the soliton.

Thus to zero order the stationary soliton energy $W_0 = 2A_0{}^2\tau$ is determined by the condition that the saturated gain is equal to the total loss attributable to the linear loss l, gain filtering, and modulator loss:

$$g - l = \frac{\pi^2}{24}M\omega_M{}^2\tau^2 + \frac{g}{3\Omega_g{}^2\tau^2} , \tag{3.2}$$

with the saturated gain

$$g = \frac{g_0}{1 + W_0/E_L} . \tag{3.3}$$

Linearization around this stationary value gives for the soliton perturbations

$$T_R \frac{\partial \Delta W}{\partial T} = 2\Bigg[-\frac{g}{(1 + W_0/E_L)}\left(\frac{W_0}{E_L} + \frac{1}{3\Omega_g{}^2\tau^2}\right) + \frac{\pi^2}{12} M\omega_M{}^2\tau^2\Bigg]\Delta W + \langle \mathbf{f}_w^{(+)} | \mathbf{R}\mathbf{a}_c\rangle, \quad (3.4)$$

$$T_R \frac{\partial \Delta\theta}{\partial T} = \langle \mathbf{f}_\theta^{(+)} | \mathbf{R}\mathbf{a}_c\rangle, \quad (3.5)$$

$$T_R \frac{\partial \Delta p}{\partial T} = -\frac{4g}{3\Omega_g{}^2\tau^2}\Delta p + \langle \mathbf{f}_p^{(+)} | \mathbf{R}\mathbf{a}_c\rangle, \quad (3.6)$$

$$T_R \frac{\partial \Delta t}{\partial T} = -\frac{\pi^2}{4} M\omega_M{}^2\tau^2\Delta t - 2|D|\Delta p + \langle \mathbf{f}_t^{(+)} | \mathbf{R}\mathbf{a}_c\rangle, \quad (3.7)$$

and for the continuum we obtain

$$T_R \frac{\partial g(k)}{\partial T} = -i\Phi_0(k^2 + 1)g(k) + \langle \mathbf{f}_k^{(+)} | \mathbf{R}\mathbf{a}_c\rangle + \langle \mathbf{f}_k^{(+)} | \mathbf{R}[\mathbf{a}_0(x) + \Delta w\mathbf{f}_w + \Delta p\mathbf{f}_p]\rangle - \langle \mathbf{f}_k^{(+)} | M\omega_M \sin(\omega_M\tau x)\mathbf{a}_0(x)\rangle\Delta t. \quad (3.8)$$

Thus the action of the active mode locker and gain dispersion has several effects. First, the mode locker leads to a restoring force in the timing of the soliton [Eq. (3.7)]. Second, the gain dispersion and the active mode locker lead to coupling between the perturbed soliton and the continuum, which results in steady excitation of the continuum.

However, we will see below that the pulse width of the soliton, which can be stabilized by the mode locker, is not too far from the Gaussian pulse width as a result of active mode locking alone [Eq. (2.12)]. Then relation

$$\omega_M\tau \ll 1 \ll \Omega_g\tau \quad (3.9)$$

is fulfilled. The weak gain dispersion and the weak active mode locker only couple the soliton to the continuum, but to first order the continuum does not couple back to the soliton. Neglecting higher-order terms in the matrix elements of Eq. (3.8) (see Appendix A) results in a decoupling of the soliton perturbations from the continuum in Eqs. (3.4)–(3.8). For a laser far above threshold, i.e., $W_0/E_L \gg 1$, gain saturation always stabilizes the amplitude perturbation, and Eqs. (3.5)–(3.7) indicate stability for phase, frequency, and timing fluctuations. This is in contrast to the situation in a soliton storage ring in which the laser amplifier compensating for the loss in the ring is below threshold.[11]

By inverse Fourier transformation of Eq. (3.8) and weak coupling, we obtain for the associated function of the continuum

$$T_R \frac{\partial G}{\partial T} = \Bigg\{ g - l - i\Phi_0 + \frac{g}{\Omega_g{}^2}(1 + iD_n)\frac{\partial^2}{\partial t^2} - M[1 - \cos(\omega_M t)]\Bigg\} G + \mathcal{F}^{-1}[\langle \mathbf{f}_k^{(+)} | \mathbf{R}\mathbf{a}_0(x)\rangle - \langle \mathbf{f}_k^{(+)} | M\omega_M \sin(\omega_M\tau x)\mathbf{a}_0(x)\rangle\Delta t], \quad (3.10)$$

where D_n is the dispersion normalized to the gain dispersion:

$$D_n = |D|\Omega_g{}^2/g. \quad (3.11)$$

Note that the homogeneous part of the equation of motion for the associated function of the continuum, which governs the decay of the continuum, is the same as the homogeneous part of the equation for the noise in a soliton storage ring at the position where no soliton or bit is present.[11] Thus the decay of the continuum is not affected by the nonlinearity, but there is a continuous excitation of the continuum by the soliton when the perturbing elements are passed by the soliton. Thus under the above approximations the question of stability of the soliton solution is completely governed by the stability of the continuum [Eq. (3.10)]. As we can see from Eq. (3.10), the evolution of the continuum obeys the active mode-locking equation with GVD but with a value for the gain determined by Eq. (3.2). In the parabolic approximation of the cosine we again obtain the Hermite Gaussians [Eq. (2.11)] as the eigensolutions for the evolution operator, but the width of these eigensolutions is now given by

$$\tau_c = \tau_a \sqrt[4]{(1 + iD_n)}, \quad (3.12)$$

and the associated eigenvalues are

$$\lambda_m = -i\Phi_0 + g - l - M\omega_M{}^2\tau_a{}^2\sqrt{(1 + iD_n)}(m + 1/2). \quad (3.13)$$

The gain is clamped to the steady-state value given by condition (3.2), and we obtain

$$\lambda_m = -i\Phi_0 + \frac{1}{3}\sqrt{D_g M_s}\Bigg[\left(\frac{\tau_a}{\tau}\right)^2 + \frac{\pi^2}{4}\left(\frac{\tau_a}{\tau}\right)^{-2} - 6\sqrt{(1 + iD_n)}(m + 1/2)\Bigg]. \quad (3.14)$$

Stability is achieved when all continuum modes see a net loss per round trip, $\mathrm{Re}\{\lambda_m\} < 0$ for $m \geq 0$; i.e., we get from Eq. (3.14)

$$\left(\frac{\tau_a}{\tau}\right)^2 + \frac{\pi^2}{4}\left(\frac{\tau}{\tau_a}\right)^2 < 3\ \mathrm{Re}\{\sqrt{(1 + iD_n)}\}. \quad (3.15)$$

Inequality (3.15) establishes a quadratic inequality for the pulse-width reduction ratio $\xi = (\tau_a/\tau)^2$, which is a measure for the pulse-width reduction that is due to soliton formation:

$$\xi^2 - 3\ \mathrm{Re}\{\sqrt{(1 + iD_n)}\}\xi + (\pi^2/4) < 0. \quad (3.16)$$

As has to be expected, this inequality can be satisfied only if we have a minimum amount of negative normalized dispersion so that a soliton can be formed at all:

$$D_{n,\mathrm{crit}} = 0.652. \quad (3.17)$$

Therefore our perturbation ansatz gives meaningful results only beyond this critical amount of negative dispersion. Because ξ compares the width of a Gaussian with

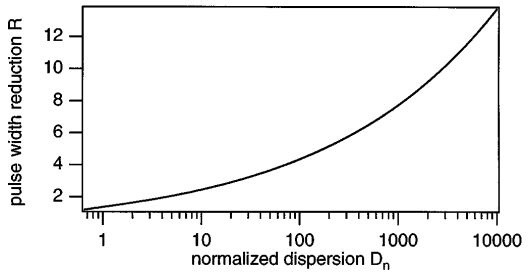

Fig. 1. Pulse-width reduction as a function of normalized dispersion. Below $D_{n,\mathrm{crit}} = 0.652$ no stable soliton can be formed.

that of a hyperbolic secant, it is more relevant to compare the full width at half-maximum of the intensity profiles[1] of the corresponding pulses, which is given by

$$R = \frac{1.66}{1.76}\sqrt{\xi}\,. \tag{3.18}$$

Figure 1 shows the maximum pulse-width reduction R allowed by the stability criterion [inequality (3.16)] as a function of normalized dispersion. The critical value for the pulse-width reduction is $R_{\mathrm{crit}} \approx 1.2$. For large normalized dispersion Fig. 1 shows that the soliton can be kept stable at a pulse width reduced as much as a factor of 5 when the normalized dispersion can reach a value of 100. Even at a moderate negative dispersion of $D_n = 5$ we can achieve a pulse-width reduction by a factor of 2. For large normalized dispersion the stability criterion [inequality (3.16)] approaches asymptotically the behavior

$$\xi < \sqrt{\frac{9D_n}{2}} \quad \text{or} \quad R < \frac{1.66}{1.76}\sqrt[4]{\frac{9D_n}{2}}\,. \tag{3.19}$$

Thus the possible pulse-width reduction scales with the fourth root of the normalized dispersion, indicating the need for an excessive amount of dispersion to maintain a stable soliton while suppressing the continuum. The physical reason for this is that gain filtering and the active mode locker continuously shed energy from the soliton into the continuum. For the soliton the action of GVD and SPM is always in balance and maintains the pulse shape. However, as can be seen from Eq. (3.10), the continuum, which can be viewed as a weak background pulse, does not experience SPM once it is generated and therefore gets spread by GVD. This is also the reason why the eigenstates of the continuum consist of long chirped pulses that also scale with the fourth root of the dispersion [Eq. (3.12)]. Then the long continuum pulses suffer much higher loss in the active modulator, unlike the short soliton, which suffers reduced gain when it passes the gain medium because of its broader spectrum. The soliton is stable as long as the continuum sees less round-trip gain than the soliton does.

In principle, by introducing a large amount of negative dispersion the theory would predict arbitrarily short pulses. However, the master equation (2.1) describes the laser system properly only when the nonlinear changes of the pulse per pass are small. This gives an upper limit to the nonlinear phase shift Φ_0 that the soliton can undergo during one round trip. A conservative estimation of this upper limit is $\Phi_0 = 0.1$. Then the action of the individual operators in Eq. (2.1) can still be considered continuous. Even if one considers larger values for the maximum phase shift allowed, because in fiber lasers the action of GVD and SPM occurs simultaneously and therefore Eq. (2.1) may describe the laser properly even for large nonlinear phase shifts per round trip, one will run into intrinsic soliton and sideband instabilities for Φ_0 approaching 2π.[16,18,19] Under the condition of a limited phase shift per round trip we obtain from Eq. (2.7)

$$\tau^2 = |D|/\Phi_0\,. \tag{3.20}$$

Thus, from Eq. (2.17), the definition of ξ, inequality (3.19), and Eq. (3.20), we obtain for the maximum possible reduction in pulse width

$$R_{\max} = \frac{1.66}{1.76}\sqrt[12]{\frac{(9\Phi_0/2)^2}{D_g M_s}} \tag{3.21}$$

and therefore for the minimum pulse width

$$\tau_{\min} = \sqrt[6]{\frac{2D_g{}^2}{9\Phi_0 M_s}}\,. \tag{3.22}$$

The necessary amount of normalized negative GVD is then given by

$$D_n = \frac{2}{9}\sqrt[3]{\frac{(9\Phi_0/2)^2}{D_g M_s}}\,. \tag{3.23}$$

Equations (3.21)–(3.23) constitute the main results of this paper, because they allow us to compute the possible pulse-width reduction and the necessary negative GVD for a given laser system. Table 1 shows the evaluation of these formulas for several gain media and typical laser parameters. It shows that soliton formation in actively mode-locked lasers may lead to considerable pulse shortening, up to a factor of 10 in Ti:sapphire. Because of the 12th root in Eq. (3.21) the shortening depends mostly on the bandwidth of the gain material, which can change by

Table 1. Maximum Pulse-Width Reduction and Necessary Normalized GVD for Different Laser Systems[a]

Gain Material	$\frac{\Omega_g}{2\pi}$ (THz)	M	$\frac{\omega_M}{2\pi}$ (MHz)	$\frac{D_g}{(\mathrm{ps}^2)}$	M_s (ps^2)	$\frac{\tau_{a,\mathrm{FWHM}}}{(\mathrm{ps})}$	$R_{\max}$	$\frac{T_{\min,\mathrm{FWHM}}}{(\mathrm{ps})}$	D_n	$\frac{\tau_{\mathrm{trans}}}{T_R}$
Nd:YAG	0.06	0.2	250	0.7	2.5×10^{-7}	68	3	22.7	23.4	702
Nd:glass	4	0.2	250	158×10^{-6}	2.5×10^{-7}	8.35	6	1.4	385	11,538
Cr:LiSAF	32	0.2	250	2.4×10^{-6}	2.5×10^{-7}	3	8.6	0.35	1563	46,600
Ti:sapphire	43	0.01	100	1.4×10^{-6}	2×10^{-9}	8.5	13.5	0.63	9367	281,000

[a] In all cases we used for the saturated gain $g = 0.1$ and for the soliton phase shift per round trip $\Phi_0 = 0.1$. For the broadband gain materials the last column indicates rather long transient times, which call for regenerative mode locking.

Table 2. Parameters Used for Numerical Simulations

Parameter	Value
l	0.1
g_0	1
P_L	1 W
Ω_g	$2\pi \times 60$ GHz
ω_M	$2\pi \times 0.25$ GHz
T_R	4 ns
M	0.2
δ	1.4×10^{-4} W^{-1}
D	-17 ps^2/-10 ps^2

several orders of magnitude for the different laser materials. The amount of negative dispersion required for achieving this additional pulse shortening is in a range that can be achieved by gratings, Gires–Tournois interferometers, or prisms.

Of course, in the experiment one has to stay away from these limits to suppress the continuum sufficiently. However, as numerical simulations show, the transition from stable to unstable behavior is remarkably sharp. The reason for this can be understood from the structure of the eigenvalues for the continuum [Eq. (3.14)]. The time scale for the decay of transients is given by the inverse of the real part of the fundamental continuum mode, which diverges at the transition to instability. Nevertheless, a good estimate for this transient time is given by the leading term of the real part of Eq. (3.14):

$$\frac{\tau_{\text{trans}}}{T_R} = \frac{1}{\text{Re}\{\lambda_0\}} \approx \frac{3}{\sqrt{D_g M_s}\, R^2}\,. \tag{3.24}$$

This transient time is also shown in Table 1 for different laser systems. Thus these transients decay, if they are not too close to the instability border, on time scales from approximately 1000 to some 100,000 round trips, depending strongly on the gain bandwidth and the modulation strength. Consequently, to first order, the eigenvalues of the continuum modes, which are excited by the right-hand side of Eq. (3.10), are purely imaginary and independent of the mode number; i.e., $\lambda_n \approx -i\Phi_0$. Therefore, as long as the continuum is stable, the solution to Eq. (3.10) is given by

$$G(x) = \frac{i}{\Phi_0}\, \mathcal{F}^{-1}\{\langle \mathbf{f}_k^{(+)} \,|\, \mathbf{R}\mathbf{a}_0(\mathbf{x})\rangle - M_s \tau^2 \langle \mathbf{f}_k^{(+)} \,|\, x\mathbf{a}_0(x)\rangle (\Delta t/\tau)\}\,. \tag{3.25}$$

Thus in steady state the continuum is of the order of

$$|G(x)| \approx \frac{A_0}{\Phi_0}\,\frac{D_g}{\tau^2} = \frac{A_0}{D_n}\,, \tag{3.26}$$

which again demonstrates the spreading of the continuum by the dispersion. This shows that the nonlinear phase shift of the solitary pulse per round trip has to be chosen as large as possible, which also maximizes the normalized dispersion, so that the radiation shed from the soliton into the continuum changes the phase rapidly enough that the continuum in steady state stays small. Note that the size of the generated continuum according to relation (3.26) is largely independent of the real part of the lowest eigenvalue of the continuum mode. Therefore the border to instability is sharply defined. However, the time scale of the transients at the transition to instability can become arbitrarily long. Therefore numerical simulations are trustworthy only if the time scales for transients in the system are known from theoretical considerations such as those derived above in relation (3.24). The simulation time for a given laser should be at least of the order of 10 times τ_{trans} but even longer for operation close to the instability point, as we will see in Section 4.

4. NUMERICAL SIMULATIONS

In this section we compare the theory developed above with numerical simulations. A Nd:YAG laser is chosen for our example because of its moderate gain bandwidth and therefore its large gain dispersion. This will limit the possible pulse-width reduction to ~3, but the decay time of the continuum [relation (3.4); see also Table 1] is then in a range of 700 round trips so the steady state of the mode-locked laser can be reached with moderate computer time, while the approximations involved [inequality (3.19)] are still satisfied. The system parameters used for the simulation are given in Table 2. Without GVD and SPM we would obtain a Gaussian pulse with a FWHM according to Eqs. (2.12) and (2.17) of

$$\tau_{a,\text{FWHM}} = 68 \text{ ps}\,, \tag{4.1}$$

where we have assumed that the saturated gain is equal to the loss l. Allowing for a maximum nonlinear phase shift $\Phi_0 = 0.1$ in Eq. (3.23) we obtain for the normalized dispersion $D_n = 23.4$ and therefore a maximum reduction in pulse width [Eq. (3.18)] of $R = 3$.

For the simulation of Eq. (2.1) we use the standard split-step Fourier-transform method. Here we include the discrete action of SPM and GVD per round trip by choosing the integration step size for the T integration to be the round-trip time T_R. We used a discretization of 1024 points over the bandwidth of 1 THz, which corresponds to a resolution in the time domain of 1 ps. All the following figures show only one tenth of the simulated window in time and frequency.

Figure 2 shows the result of the simulation starting with a 68-ps-long Gaussian pulse with a pulse energy of

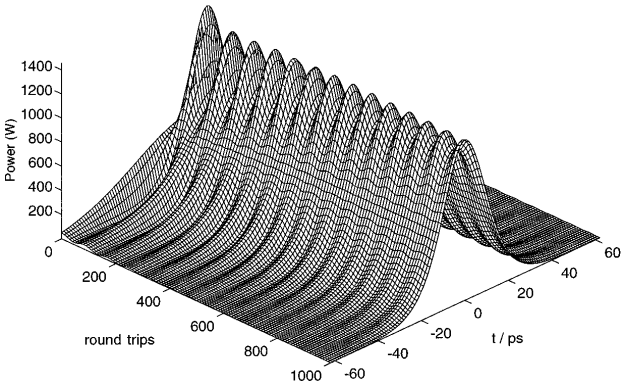

Fig. 2. Time evolution of the pulse intensity in a Nd:YAG laser for the parameters in Table 2, $D = -17$ ps^2, for the first 1,000 round trips in the laser cavity, starting with a 68-ps-long Gaussian pulse.

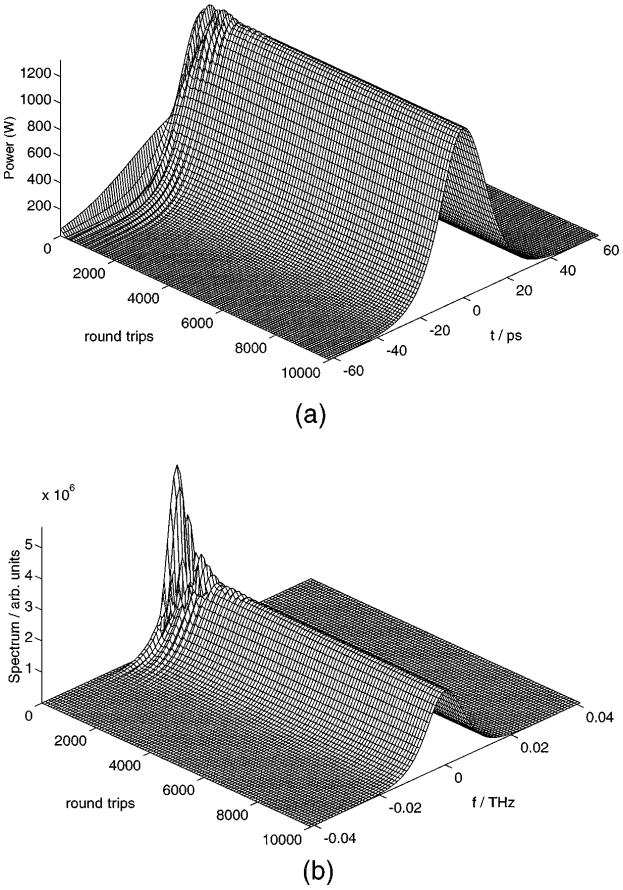

Fig. 3. Time evolution of (a) the intensity and (b) the spectrum for the same parameters as in Fig. 2 over 10,000 round trips. The laser reaches steady state after ~4000 round trips.

$W = 40$ nJ for $D_n = 24$, i.e., $D = -17$ ps^2. For the given SPM coefficient this should lead to stable pulse shortening by a factor of $R = 2.8$. Thus after at least a few thousand round trips the laser should be in steady state again with a FWHM pulse width of 24 ps. Figure 2 shows the pulse evolution over the first 1,000 round trips, i.e., 4-μs real time. The long Gaussian pulse at the start contains an appreciable amount of continuum. As we can see from Eqs. (2.17), (2.55), and (3.14), the continuum part of the solution, in contrast to the soliton, does not experience the nonlinear phase shift that is due to SPM. Thus the soliton interferes with the continuum periodically, with a soliton period of $T_{\text{soliton}}/T_R = 2\pi/\Phi_0 = 20\pi$. This is the reason for the oscillations of the pulse amplitude seen in Fig. 2 that vanish with the decay of the continuum. Note also that the solitary pulse is formed rapidly because of the large nonlinear phase shift per round trip. Figure 3 shows the simulation in time and frequency domain over 10,000 round trips. The laser reaches steady state after ~4,000 round trips, which corresponds to $6 \times \tau_{\text{trans}}$, and the final pulse width is 24 ps, in exact agreement with the predictions of the analytic formulas derived above.

The lower normalized dispersion of $D_n = 15$ or $D = -10$ ps^2 allows for a reduction in pulse width by only $R = 2.68$. However, using the same amount of SPM as before, we leave the range of stable soliton generation. Figure 4, like Fig. 2, shows the first 1,000 round trips in that case. Again the solitary pulse is rapidly formed out of the long Gaussian initial pulse. But, in contrast to the situation for Fig. 2, the continuum no longer decays on this time scale. The dispersion is too low to spread the continuum rapidly enough. The continuum then accumulates over many round trips, as can be seen from Fig. 5. After ~10,000 round trips the continuum has grown so much that it extracts an appreciable amount of energy from the soliton. But surprisingly the continuum modes stop growing after ~30,000 round trips, and a new quasi-stationary state is reached.

Qualitatively this quasi-stationary state corresponds to the coexistence of a soliton with an appreciable amount of continuum. The soliton still interferes with the continuum, leading to periodic oscillation of the peak value. The pulse shape is no longer symmetric, because even and odd eigensolutions of the continuum are now above threshold, leading to symmetry breaking. Thus the total pulse shown in Fig. 5 looks like a 50-ps long pulse followed by a 24-ps short pulse, a phenomenon that one observes experimentally when leaving the stability regime, as discussed in Section 5.

These are only qualitative remarks because for a quantitative analysis the theory presented above would have to be carried further to second-order perturbation theory to yield the amplitudes of the continuum excitations beyond the stability range derived in Subsection 2.C. That study is beyond the scope of this paper, however.

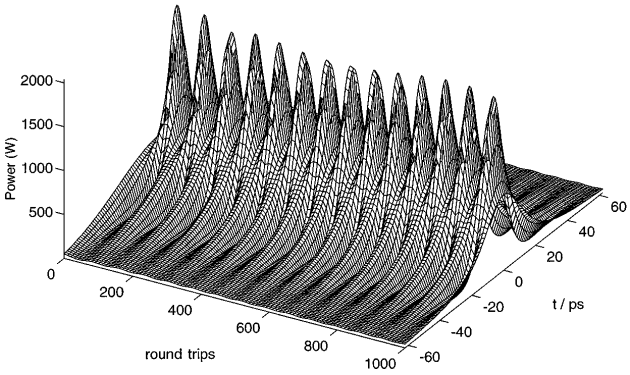

Fig. 4. Time evolution of the intensity in a Nd:YAG laser for the parameters in Table 2. The amount of negative dispersion is reduced to $D = -10$ ps^2, starting again from a 68-ps-long pulse. The continuum in this case does not decay as in Figs. 2 and 3 because of insufficient dispersion.

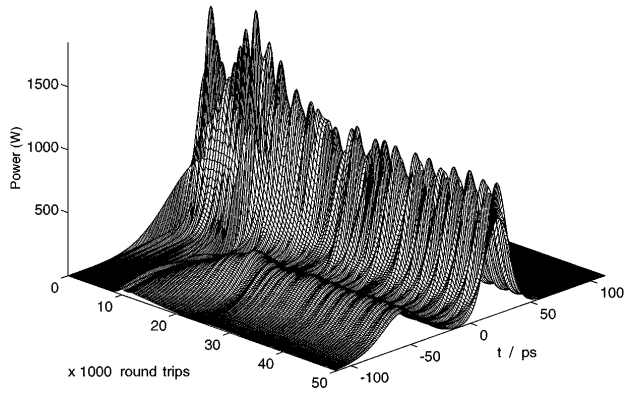

Fig. 5. Parameters chosen as for Fig. 4 but for 50,000 round trips.

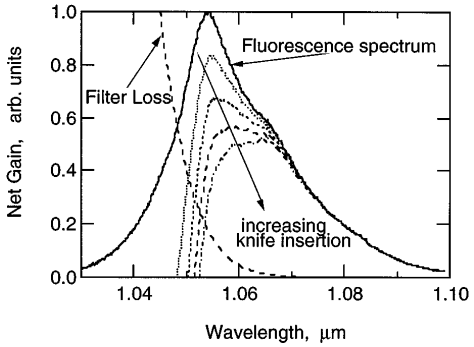

Fig. 6. Solid curves, the normalized fluorescence spectrum of the Nd:glass LG-760 used in our experiment, measured with an optical spectrum analyzer, when pumped below threshold. LG-760 is a quasi-homogeneous laser material; thus when it is lasing the saturated gain is proportional to the fluorescence spectrum. From the refractive index of the quartz prism and the beam waist at the knife position we can calculate the low-path filter function attributable to the knife-edge relative to the knife position, which is an error function. The several dashed curves show the difference between the saturated gain determined from the measured fluorescence spectrum and the computed low-path filter losses for different knife positions, which we call the net gain. For lasing at a certain power level, moving the knife edge into the cavity reduces the overall gain somewhat but also flattens the net gain profile over a range of ~10 nm.

5. EXPERIMENTAL RESULTS

The Nd:YAG laser is not a proper candidate for verification of the theory experimentally, because the necessary large amount of negative dispersion to achieve soliton formation or even a factor-of-3 pulse shortening cannot be achieved simply by a pair of prisms. However, we believe that the theory above explains very well the picosecond Ti:sapphire experiments[5] in the regime where the pulses are stabilized by the active mode locker alone. Gires–Tournois interferometers were used to produce large amounts of negative GVD to operate the laser in the stable soliton regime derived above. Here we discuss in more detail the experimental results obtained recently with a regeneratively actively mode-locked Nd:glass laser,[6] which resulted in generation of 310 fs pulses. The Nd:glass laser system is interesting because of its potential for ultrashort-pulse generation owing to the large gain bandwidth available[8] and because it can be diode pumped.[9]

We used a standard dispersion-compensated delta cavity,[20] in which an intracavity filter formed by a knife-edge introduced between the prisms for dispersion compensation allows for a modification of the net gain profile of the laser and therefore for a variation in the effective gain bandwidth.[6] The high-Q acousto-optic modulator was operated off resonance as a regenerative mode locker and therefore had a modulation depth of only $M = 0.01$. Figure 6 shows the fluorescence spectrum of the phosphate Nd:glass material LG-760. If we do not introduce a knife-edge, the gain bandwidth of the Nd:glass can be extracted around the peak of the fluorescence spectrum to be $\Omega_g = 25$ THz. The laser beam was tightly focused into the gain medium, resulting in a self-phase modulation coefficient of $\delta = 0.4/\mathrm{MW}$. The repetition rate was $f_M = 250$ MHz, the total cavity losses are 2%, and therefore $g \approx 1\%$. Note that the quantities in the master equation (2.1) are related to amplitude and not to power. The output coupling was 1%. The output power varied from 70 to 150 mW, depending on the position of the knife-edge. The total amount of negative dispersion available in this setup was limited to $D \approx 1300\ \mathrm{fs}^2$. If SPM and GVD could be neglected, the weak mode locker would produce Gaussian pulses with a FWHM of $\tau_{a,\mathrm{FWHM}} = 10$ ps. However, the strong SPM prevents stable pulse formation.[1] The negative dispersion available in the experiment is too low to permit stable soliton formation, because the pulse width of the soliton at this power level is given by $\tau = 4|D|/(\delta W) = 464$ fs. Therefore the normalized dispersion is not large enough to allow for such a large pulse-width reduction, as can be seen from inequality (3.19) and Fig. 1, because $D_{n,\max} = 23$ in that case. However, moving the knife-edge into the beam, which acts as a long-path wavelength filter, results in a new net gain profile that is flat over ~10 nm.

Obviously, the net gain profile can no longer be fitted to a parabola. However, it is instructive to follow what happens when the gain parabola is gradually opened up by insertion of the knife-edge. Suppose that we increase the gain bandwidth by a factor of 9. The actively mode-locked pulse width of the purely Gaussian pulses is then reduced by only a factor of $\sqrt{9} = 3$, to $\tau_{a,\mathrm{FWHM}} = 3.3$ ps. But at the same time the maximum normalized dispersion increases with the square of the bandwidth to $D_{n,\max} = 1863$, which would allow for an additional pulse shortening attributable to soliton formation by a factor of 9 (see Fig. 1), resulting in a 370-fs short and most importantly stable solitonlike pulse. Of course the flattening process shown in Fig. 6 is not well described by a parabola. Thus soliton formation essentially allows us to fill up the flat part of the net gain profile, which could never be achieved by the weak mode locker alone. This results in a 310-fs perfectly sech-shaped solitonlike pulse, as shown in Fig. 7, which corresponds to a bandwidth of ~3 nm. We observed no contribution from Kerr-lens mode locking, as switching off the drive signal to the acousto-optic modulator resulted in a cw running laser.

A numerical simulation of this case would need millions of round trips through the cavity until a stationary state is reached. This means milliseconds of real time but would necessitate days of computer time.

We also observed in the transition to unstable behavior the characteristic occurrence of a short, solitary femtosecond pulse together with a long, picosecond pulse as a result of the instable continuum, as we have found in

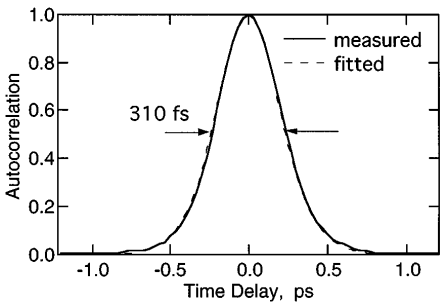

Fig. 7. Autocorrelation of the mode-locked pulse (solid curve) and the corresponding sech^2 fit (dashed curve). The output power was 70 mW at 930-mW absorbed pump power.

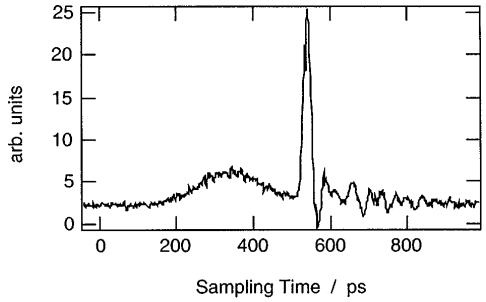

Fig. 8. Sampling signal of the fast detector when the mode-locked laser operates at the transition to instability. The short, femtosecond pulse cannot be resolved by the detector and therefore results in a sharp spike corresponding to the detector response time. In advance of the femtosecond pulse there is a roughly 100-ps-long pulse.

the numerical simulation for the case of a Nd:YAG laser (see Fig. 5). Figure 8 shows the signal of a fast detector diode on the sampling oscilloscope. The detector has an overall bandwidth of 25 GHz and therefore cannot resolve the femtosecond pulse but can resolve the width of the following roughly 100-ps-long pulse. According to the theory, the time scale of the continuum modes is of the order of $\mathrm{Re}(\tau_{c,\mathrm{FWHM}}) \approx \tau_{a,\mathrm{FWHM}} \cos(45°) \sqrt[4]{D_n} = 35$ ps, where we have used a value for the normalized dispersion of $D_n = 10,000$. Therefore the observed double pulsing in the actively mode-locked laser at the transition to instability can be explained if we assume that a few lower-order Hermite Gaussian continuum modes are above threshold but still not far enough above threshold to take too much of the energy away from the solitary pulse.

6. CONCLUSIONS

We extended the early investigations of Haus and Silberberg on pulse shortening,[1] using SPM and GVD in actively mode-locked lasers, and found that beyond a critical value of negative GVD a stable solitary pulse can indeed be formed and kept stable by the mode locker. We derived analytical expressions for the possible stability range and the pulse shortening. The pulse shortening achieved by these means can be as large as a factor of 10 for the case of Ti:sapphire. If we choose optimum values for a Nd:glass laser without gain reshaping, the usual 8–10-ps-long pulses in an active mode-locking experiment[8] can be shortened by a factor of $R = 6$ to $\tau_{\mathrm{FWHM}} = 1.4$ ps according to Table 1 if the laser is operated in the soliton regime by introduction of a dispersion compensation that produces a total intracavity negative GVD of $D = -61 \times 10^3$ fs^2. Thus this technique allows for considerable pulse shorting in actively mode-locked Nd:glass lasers. Application of additional intracavity filtering allows reaching even the femtosecond regime. However, it reduces the output power as a result of additional intracavity losses.

The main result of this paper, that a soliton that is much shorter than the Gaussian pulse because of pure active mode locking can be stabilized by an active mode locker, also has an important consequence for passive mode locking. It implies that a slow saturable absorber, i.e., an absorber with a recovery time much longer than the width of the soliton, is enough to stabilize the pulse, i.e., to mode lock the laser. However, this subject will be pursued in a forthcoming publication.[21]

APPENDIX A

In this appendix we prove that the mode locker and the gain filtering only weakly couple the soliton to the continuum, which allows for Eq. (3.8). From the soliton perturbation theory outlined in Subsection 2.6 we obtain for the matrix element coupling the continuum and the soliton

$$\langle \mathbf{f}_k^{(+)} | \cos(\omega_M \tau x) | \mathbf{f}_{k',w,\theta,p,t} \rangle = \tfrac{1}{2} \langle \mathbf{f}_k^{(+)} | [\mathbf{f}_{k-\omega_M\tau}^{(+)} + \mathbf{f}_{k+\omega_M\tau}^{(+)} + O(\omega_M \tau)] | \mathbf{f}_{k',w,\theta,p,t} \rangle ,$$

where we have made use of the fact that the eigenfunctions of the continuous spectrum are plane waves outside the interaction zone, Eq. (3.25), with the soliton and there the active mode locker has the most action on the waves. Thus we get

$$\langle \mathbf{f}_k^{(+)} | \cos(\omega_M \tau x) | \mathbf{f}_{k'} \rangle = \tfrac{1}{2} [\delta(k - k' + \omega_M \tau) + \delta(k - k' - \omega_M \tau)] + O(\omega_M \tau) , \tag{A1a}$$

$$\langle \mathbf{f}_k^{(+)} | \cos(\omega_M \tau x) | \bar{\mathbf{f}}_{k'} \rangle = O(\omega_M \tau) , \tag{A1b}$$

$$\langle \bar{\mathbf{f}}_k^{(+)} | \cos(\omega_M \tau x) | \mathbf{f}_{k'} \rangle = \tfrac{1}{2} [\delta(k - k' + \omega_M \tau) + \delta(k - k' - \omega_M \tau)] + O(\omega_M \tau) , \tag{A1c}$$

$$\langle \bar{\mathbf{f}}_k^{(+)} | \cos(\omega_M \tau x) | \mathbf{f}_{k'} \rangle = O(\omega_M \tau) ; \tag{A1d}$$

$$\langle (\mathbf{f}, \bar{\mathbf{f}})_k^{(+)} | \cos(\omega_M \tau x) | \mathbf{f}_{w,\theta,p,t} \rangle = O(\omega_M \tau) , \tag{A1e}$$

$$\langle \mathbf{f}_{w,\theta,p,t}^{(+)} | \cos(\omega_M \tau x) | (\mathbf{f}, \bar{\mathbf{f}})_k \rangle = O(\omega_M \tau) . \tag{A1f}$$

Similar relations can be obtained for the matrix elements of the gain dispersion operator:

$$\langle \mathbf{f}_k^{(+)}(x) | F\left(\frac{1}{\Omega_g \tau} \frac{\partial}{\partial x} \right) | \mathbf{f}_{k',w,\theta,p,t}(x) \rangle , \tag{A2}$$

where $F(y)$ is a function that does not vary strongly. Then we obtain for the matrix element [expression (A2)] in the Fourier representation

$$\langle \mathbf{f}_k^{(+)}(\omega) | F\left(\frac{i\omega}{\Omega_g \tau} \right) | \mathbf{f}_{k',w,\theta,p,t}(\omega) \rangle , \tag{A3}$$

with the Fourier transform of [Eq. (2.35)]

$$\mathbf{f}_k(\omega) = 2\pi\delta(\omega - k) + \pi \frac{\omega - k}{\sinh[\pi/2(\omega - k)]} + 2k \,\mathrm{P.V.}\left\{ \frac{2}{\omega - k} + \frac{\pi}{\sinh[(\pi/2)(\omega - k)]} \right\} , \tag{A4}$$

where P.V. denotes the principal value. This shows that the continuum eigenstate f_k is a wave with a spectrum strongly localized around the wave number k. $F[i\omega/(\Omega_g \tau)]$ is a slowly varying function in ω because relation (3.9) is fulfilled. Then it is useful to expand F in a Taylor series around k, and we obtain

$$\langle \mathbf{f}_k^{(+)}(\omega)|F\left(\frac{i\omega}{\Omega_g\tau}\right)|\mathbf{f}_{k',w,\theta,p,t}(\omega)\rangle = F\left(\frac{ik}{\Omega_g\tau}\right)\langle \mathbf{f}_k^{(+)}(\omega)|\mathbf{f}_{k',w,\theta,p,t}(\omega)\rangle + F'\left(\frac{ik}{\Omega_g\tau}\right)\langle \mathbf{f}_k^{(+)}(\omega)|(\omega)|(\omega-k)|\mathbf{f}_{k',w,\theta,p,t}(\omega)\rangle + \ldots . \quad \text{(A5)}$$

If the integrals on the right-hand side of Eq. (A5) exist, we obtain

$$\langle \mathbf{f}_k^{(+)}(\omega)|F\left(\frac{i\omega}{\Omega_g\tau}\right)|\mathbf{f}_{k',w,\theta,p,t}(\omega)\rangle = F\left(\frac{ik}{\Omega_g\tau}\right)\delta(k-k') + O\left(\frac{1}{\Omega_g\tau}\right). \quad \text{(A6)}$$

Note that if $F(y)$ is only a power, as is the case in our quadratic approximation of the gain profile, the scaling factor $1/(\Omega_g\tau)^2$ can be pulled out to the front, and Eq. (A7) below is not applicable because a power is not slowly varying in the whole domain. However, the correct physical gain profile is a Lorentzian that is weakly varying in the whole domain, and then Eq. (A7) is applicable and the resulting function can again be approximated up to a second order. Thus we can replace in inequality (3.9) the matrix elements of the differential operator in $\mathbf{R}$ by

$$\langle \mathbf{f}_k^{(+)}|\frac{\partial^2}{\partial x^2}|\mathbf{f}_{k',w,\theta,p,t}(\omega)\rangle = -k^2\delta(k-k') + O\left(\frac{1}{\Omega_g\tau}\right). \quad \text{(A7)}$$

Thus the differential operator strongly couples only the same continuum modes.

ACKNOWLEDGMENTS

Thanks go to K. J. Weingarten for helping us with the regenerative mode-locking technique and to Lightwave Electronics for donating the mode locker and the drive electronics. This research was supported by the Swiss National Fund 21-39362.93.

REFERENCES

1. H. A. Haus and Y. Silberberg, "Laser mode locking with addition of nonlinear index," IEEE J. Quantum Electron. **QE-22,** 325–331 (1986).
2. J. D. Kafka and T. Baer, "Mode-locked erbium-doped fiber laser with soliton pulse shaping," Opt. Lett. **14,** 1269–1271 (1989).
3. K. Smith, R. P. Davey, B. P. Nelson, and E. J. Greer, *Fiber and Solid-State Lasers* (Institution of Electrical Engineers, London, 1992), p. 1/1-4.
4. F. Fontana, N. Ridi, M. Romagnoli, and P. Franco, "Fully integrated 30 ps modelocked fiber laser electronically tunable over 1530–1560 nm," Opt. Commun. **107,** 240–244 (1994).
5. J. D. Kafka, M. L. Watts, and J.W. J. Pieterse, "Picosecond and femtosecond pulse generation in a regeneratively mode-locked Ti:sapphire laser," IEEE J. Quantum Electron. **QE-28,** 2151–2162 (1992).
6. D. Kopf, F. X. Kärtner, and U. Keller, "Pulse shortening in a Nd:glass laser by gain reshaping and soliton formation," Opt. Lett. **19,** 2146–2148 (1994).
7. A. J. DeMaria, D. A. Stetser, and H. Heynau, "Self mode-locking of lasers with saturable absorbers," Appl. Phys. Lett. **8,** 174–176 (1994).
8. L. Yan, P.-T. Ho, C. H. Lee, and G. L. Burdge, "Generation of ultrashort pulses form a neodymium glass laser system," IEEE J. Quantum Electron. **25,** 2431–2440 (1989).
9. D. W. Hughes, M. W. Phillips, J. R. M. Barr, and D. C. Hanna, "A laser-diode-pumped Nd:glass laser: mode-locked, high power, and single frequency performance," IEEE J. Quantum Electron. **28,** 1010–1017 (1989).
10. H. A. Haus, "A theory of forced mode locking," IEEE J. Quantum Electron. **QE-11,** 323–330 (1975).
11. H. A. Haus and A. Mecozzi, "Long-term storage of a bit stream of solitons," Opt. Lett. **17,** 1500–1502 (1992).
12. V. E. Zakharov and A. B. Shabat, "Exact theory of two-dimensional self-focusing and one-dimensional self-modulation of waves in nonlinear media," Zh. Eksp. Teor. Fiz. **34,** 61–68 (1971) [Sov. Phys. JETP **34,** 62–69 (1972)].
13. D. J. Kuizenga and A. E. Siegman, "FM and AM mode locking of the homogeneous laser—Part I: Theory," IEEE J. Quantum Electron. **QE-6,** 694–708 (1970).
14. A. Mecozzi, J. D. Moores, H. A. Haus, and Y. Lai, "Soliton transmission control," Opt. Lett. **16,** 1841–1843 (1991).
15. J. P. Gordon, "Dispersive perturbations of solitons of the nonlinear Schrödinger equation," J. Opt. Soc. Am. B **9,** 91–97 (1992).
16. J. N. Elgin and S. M. J. Kelly, "Spectral modulation and the growth of resonant modes associated with periodically amplified solitons," Opt. Lett. **21,** 787–789 (1993).
17. D. J. Kaup, "Perturbation theory for solitons in optical fibers," Phys. Rev. A **42,** 5689–5694 (1990).
18. S. M. J. Kelly, "Characteristic sideband instability of periodically amplified average solitons," Electron. Lett. **28,** 806–807 (1992).
19. F. Matera, A. Mecozzi, M. Romagnoli, and M. Settembre, "Sideband instability induced by periodic power variation in long-distance fiber links," Opt. Lett. **18,** 1499–1501 (1993).
20. U. Keller, T. H. Chiu, and J. F. Ferguson, "Self-starting femtosecond mode-locked Nd:glass laser using intracavity saturable absorber," Opt. Lett. **18,** 1077 (1993).
21. F. X. Kärtner and U. Keller, "Stabilization of solitonlike pulses with a slow saturable absorber," Opt. Lett. **20,** 16–18 (1995).